

Attenuation of sinking particulate organic carbon flux through the mesopelagic ocean

Chris M. Marsay^{a,b,1,2}, Richard J. Sanders^a, Stephanie A. Henson^a, Katsiaryna Pabortsava^{a,b}, Eric P. Achterberg^{b,c}, and Richard S. Lampitt^a

^aNational Oceanography Centre, University of Southampton Waterfront Campus, European Way, Southampton, SO14 3ZH, United Kingdom; ^bOcean and Earth Science, National Oceanography Centre Southampton, University of Southampton, Southampton, SO14 3ZH, United Kingdom; and ^cGEOMAR Helmholtz Centre for Ocean Research, 24148 Kiel, Germany

Edited by David M. Karl, University of Hawaii, Honolulu, HI, and approved December 9, 2014 (received for review August 8, 2014)

The biological carbon pump, which transports particulate organic carbon (POC) from the surface to the deep ocean, plays an important role in regulating atmospheric carbon dioxide (CO₂) concentrations. We know very little about geographical variability in the remineralization depth of this sinking material and less about what controls such variability. Here we present previously unpublished profiles of mesopelagic POC flux derived from neutrally buoyant sediment traps deployed in the North Atlantic, from which we calculate the remineralization length scale for each site. Combining these results with corresponding data from the North Pacific, we show that the observed variability in attenuation of vertical POC flux can largely be explained by temperature, with shallower remineralization occurring in warmer waters. This is seemingly inconsistent with conclusions drawn from earlier analyses of deep-sea sediment trap and export flux data, which suggest lowest transfer efficiency at high latitudes. However, the two patterns can be reconciled by considering relatively intense remineralization of a labile fraction of material in warm waters, followed by efficient downward transfer of the remaining refractory fraction, while in cold environments, a larger labile fraction undergoes slower remineralization that continues over a longer length scale. Based on the observed relationship, future increases in ocean temperature will likely lead to shallower remineralization of POC and hence reduced storage of CO₂ by the ocean.

biological carbon pump | particulate organic carbon | remineralization | mesopelagic

Atmospheric carbon dioxide (CO₂) levels are strongly influenced by the production, sinking, and subsequent remineralization of particulate organic carbon (POC) in the ocean (1), with the atmospheric concentration partially set by the depth at which regeneration occurs (2). Numerous studies have endeavored to describe the complex interactions that produce the typically observed depth profile of sinking POC flux attenuation as relatively simple mathematical forms (3–6), with perhaps the most commonly used being a power law equation:

$$f_z = f_{z_0} (z/z_0)^{-b} \quad [1]$$

where f_z is the flux at depth z , normalized to flux at some reference depth, z_0 , and b is the coefficient of flux attenuation (7). This relationship was originally derived from POC flux measurements from several eastern North Pacific locations, and an open ocean composite b value of 0.86 was calculated (7), a value which has since been used extensively in biogeochemical models (8) and to normalize fluxes measured in different regions and at different depths (9, 10). Regional variations in b , from 0.6 to 2.0, have since been demonstrated by deep-sea (>2,000 m) sediment trap studies (11, 12). More recently, mesopelagic POC flux attenuation between 150 m and 500 m depth was measured in the Vertical Transport in the Global Ocean (VERTIGO) project at two contrasting sites in the North Pacific (13), using neutrally buoyant sediment traps (NBSTs) developed

to improve the reliability of upper ocean flux measurements (14). During VERTIGO, two deployments of multiple NBSTs at station ALOHA [“A Long-term Oligotrophic Habitat Assessment”; a tropical oligotrophic site characterized by low surface chlorophyll and warm temperatures (15)] and two at station K2 [a seasonally variable mesotrophic site in the north-west Pacific subarctic gyre with relatively cold waters (15)] yielded b values of 1.25 and 1.36 and of 0.57 and 0.49, respectively (16). Community structure (17), mineral ballasting (4, 12, 18), temperature (19), and oxygen concentration (20) have all been proposed as factors important in explaining these variations in the vertical profile of organic carbon remineralization, through their influence on particle sinking speed, POC degradation rate, or both.

An alternative approach proposed to describe POC flux attenuation in the upper ocean is the use of an exponential equation (Eq. 2) that relates the flux at any depth to the flux measured at a reference depth by the remineralization length scale, z^* , defined as the depth interval over which the flux decreases by a factor of $1/e$ (5, 6, 21),

$$f_z = f_{z_0} \exp(-(z - z_0)/z^*) \quad [2]$$

This approach is advocated by some because, unlike the power law equation (Eq. 1), which is sensitive to the reference depth used, the resulting length scale is not affected by use of either the absolute depth or the depth relative to the base of the mixed layer or euphotic zone (21).

Significance

A key factor regulating the air–sea balance of carbon dioxide (CO₂) is the sinking of particles containing organic carbon from the surface to the deep ocean. The depth at which this carbon is released back into the water (remineralization) has a strong influence on atmospheric CO₂ concentration. Here we show a significant relationship between the remineralization depth of sinking organic carbon flux in the upper ocean and water temperature, with shallower remineralization in warmer waters. Our results contrast with data from deep-sea sediment traps, highlighting the importance of upper ocean remineralization to our understanding of the ocean’s biological carbon pump. Our results suggest that predicted future increases in ocean temperature will result in reduced CO₂ storage by the oceans.

Author contributions: C.M.M., R.J.S., K.P., E.P.A., and R.S.L. designed research; C.M.M. and K.P. performed research; C.M.M., S.A.H., and K.P. analyzed data; and C.M.M. wrote the paper, with input from all coauthors.

The authors declare no conflict of interest.

This article is a PNAS Direct Submission.

¹Present address: Department of Earth and Ocean Sciences, University of South Carolina, Columbia, SC 29208.

²To whom correspondence should be addressed. Email: cmarsay@geol.sc.edu.

This article contains supporting information online at www.pnas.org/lookup/suppl/doi:10.1073/pnas.1415311112/-DCSupplemental.

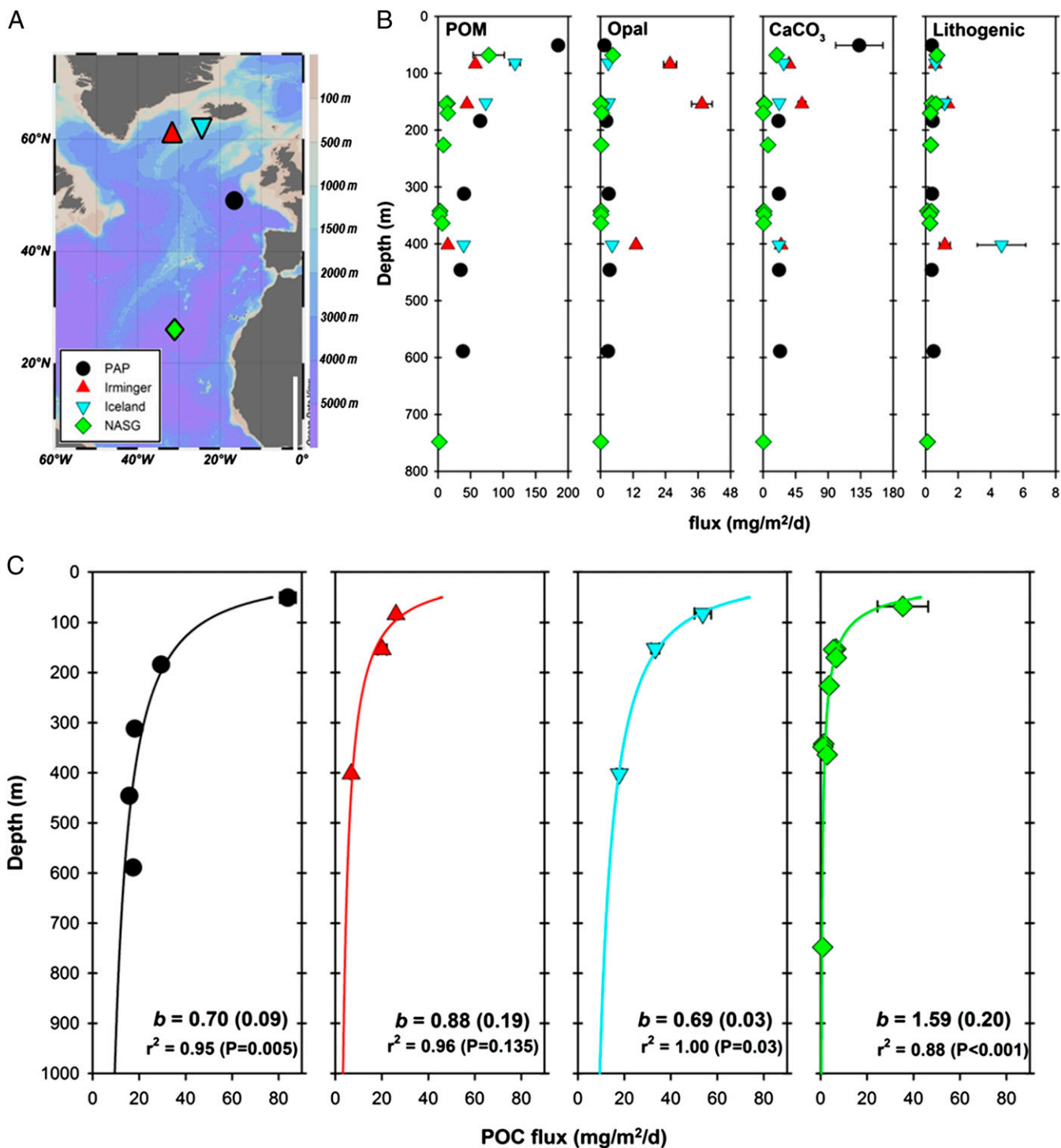


Fig. 1. (A) Bathymetry map of the North Atlantic showing the locations of four multiple PELAGRA trap deployments; (B) measured fluxes of POM, opal, CaCO_3 , and lithogenic material at each site; (C) corresponding measured POC fluxes at each site, with profiles fitted using Eq. 1 and extrapolated between 50 m and 1000 m depth. Error bars represent relative SD from replicate measurements and are generally smaller than symbols. POC flux plots show the calculated b value along with SE, r^2 value, and P value.

In this study, multiple neutrally buoyant PELAGRA (particle export measurement using a Lagrangian trap) sediment traps (22) (*SI Text*) were deployed at each of four locations in the North Atlantic: the Porcupine Abyssal Plain (PAP) time-series site, the Irminger and Iceland Basins, and within the North Atlantic subtropical gyre (NASG; Fig. 1A and Table S1). Fluxes of POC, lithogenic material, and the biominerals opal and calcium

carbonate (CaCO_3) were measured at each site (Fig. 1B and C), thereby increasing the range of locations for which these measurements have been made using NBSTs at multiple (≥ 3) depths.

Results and Discussion

At three of the study locations, particulate organic material [POM; assumed to be $2.2 \times \text{POC}$ (18)] made the greatest

contribution to mass flux of the measured phases (53–95%), with CaCO_3 also making a major contribution for most samples (<1–46%), while opal (<1–6%) and lithogenic material (<1–7%) provided only minor contributions (Fig. 1, Fig. S1, and Table S2). In contrast, at the Irminger Basin site, biominerals dominated the flux (30–46% CaCO_3 , 22–27% opal), with a lower contribution from POM (28–48%; Fig. 1, Fig. S1, and Table S2).

POC fluxes measured at each site were fitted to Eq. 1 to calculate b , yielding values of 0.70 for the PAP site (SE of 0.09), 0.88 (SE 0.19) for the Irminger Basin, 0.69 (SE 0.03) for the Iceland Basin, and 1.59 (SE 0.20) for the NASG (Fig. 1C and Table S3). The higher value of b in the Irminger Basin compared with the Iceland Basin reflects the larger percentage decrease in POC flux between 80 m and 400 m at that site (74%) compared with the Iceland Basin (67%). Nevertheless, all three b values for the more northerly sites were close to the originally proposed open ocean composite value of 0.86 (7). In contrast, the higher b value determined in the subtropical gyre reflects much greater attenuation of POC flux at that site, with a decrease of 82% between 68 m and ~160 m depth. By comparison, at the PAP site, POC flux decreased by only 65% over a similar depth interval (51 m to 184 m). As all of our estimates of b are obtained from vertical profiles of POC flux obtained entirely by using neutrally buoyant traps, the resulting methodological commonality implies that our estimates are highly internally consistent. We have thus avoided issues associated with export and transfer being measured on different time and space scales, which would introduce substantial uncertainty to the final result. For example, during previous work at the PAP site, in which estimates of export were obtained using ^{15}N and ^{234}Th , results were at times completely inconsistent with each other (22), which would have propagated large uncertainties in the value of b .

The observed difference in b values between low-latitude and midlatitude to high-latitude sites in the North Atlantic mirrors that observed in the North Pacific during the VERTIGO project. A notable feature in both ocean basins is that higher b values (i.e., shallower remineralization of sinking POC) were calculated at the stations with warmer surface and mesopelagic waters. To further investigate this relationship, we calculated the median temperature of the upper 500 m of the water column (covering the majority of the upper mesopelagic over which sampling took place) at the time of sampling for each of the eight available deployments of multiple NBSTs (the four North Atlantic study sites described here and the four VERTIGO deployments in the North Pacific). A strong correlation of mesopelagic POC flux attenuation with upper water column temperature was observed [$b = (0.062 \times T) + 0.303$; $r^2 = 0.82$, $P < 0.005$; Fig. 2A and Table S3], with depth penetration of POC being greatest in cold waters and shallower remineralization taking place in warm waters.

Using the alternative description of flux provided by Eq. 2, plotting the calculated remineralization length scale for each site (Table S3) against the same temperature metric also gives a good correlation [$z^* = 483 - (19 \times T)$; $r^2 = 0.74$, $P = 0.006$; Fig. 2B], with a trend for a longer remineralization length scale at colder sites. Thus, using either mathematical description of the vertical change in POC flux shows a strong relationship with temperature, giving us confidence that the relationship is a robust one (also see *SI Text*).

The attenuation of POC flux with depth is a product of both the remineralization rate of organic material and the sinking speed of the POC-containing particles. Faster remineralization and slower sinking both result in shallower POC remineralization. Therefore, the observed correlation between flux attenuation and temperature could arise if material exported from the surface ocean in warm regions sinks more slowly than that sinking through colder waters, thus providing more time for remineralization to take place (23). No detailed study of particle sinking velocity was carried out at the North Atlantic sites, but

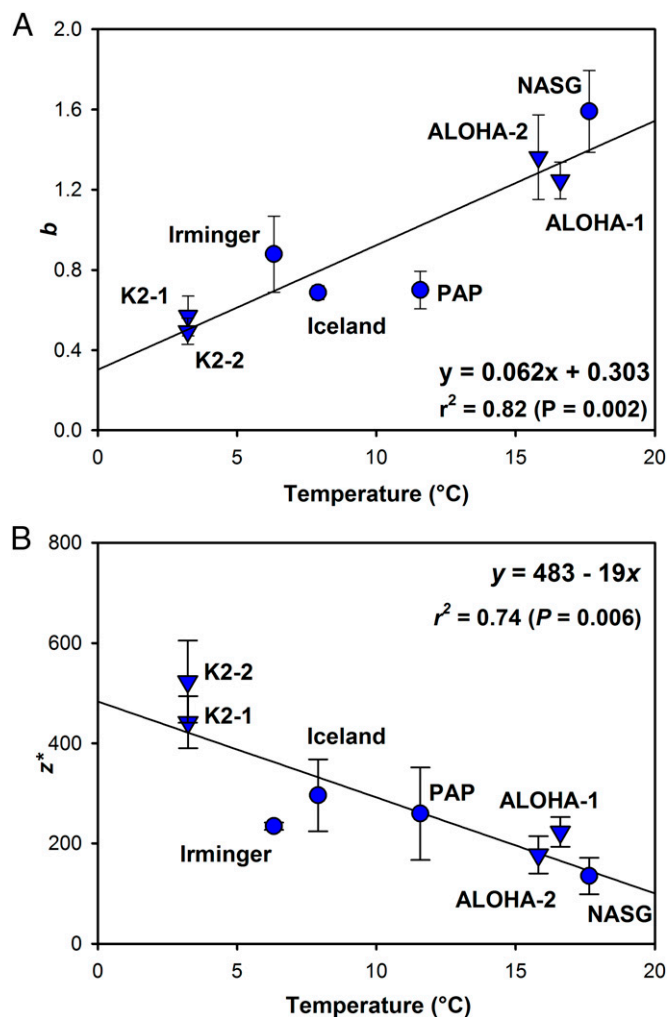


Fig. 2. Scatter plots of temperature versus (A) the b coefficient of POC flux attenuation from Eq. 1 and (B) the remineralization length scale, z^* , from Eq. 2. Values of b or z^* calculated for POC flux measurements made with neutrally buoyant sediment traps are plotted against median temperature of the upper 500 m of the water column at each site, along with the resulting regression lines. Four North Atlantic values (this study) are shown by circles; four North Pacific values (16) are shown by inverted triangles. Error bars represent SE of b and z^* values.

particle sinking rates at ~300 m depth during the VERTIGO project showed no clear difference between the warm and cold locations (24). Similarly, experiments involving aggregates of diatoms have shown no significant difference in sinking rates when carried out at 4 °C and at 15 °C (25). Alternatively, the observed relationship between flux attenuation and temperature could point to remineralization rates being the key factor in controlling flux attenuation in the upper mesopelagic, with enhanced rates in warm waters. This is consistent with other biological rate processes which, on average, scale with temperature such that a 10 °C temperature rise increases rates by a factor (the Q_{10} coefficient) of ~2–3. Notably, within the euphotic zone, heterotrophic respiration has been shown previously to have a larger Q_{10} relative to autotrophic production, resulting in reduced export of POC under warmer conditions (26, 27). Laboratory studies on diatom aggregates have also shown a 3.5-fold increase in average carbon-specific respiration rate at 15 °C relative to that at 4 °C (25).

Another possibility is that organic material exported from warm surface waters is inherently more labile than that exported

in cold regions. This is seemingly at odds with conclusions reached by combined analysis of deep ocean (>2,000 m) particle flux studies and satellite observations (12, 28). One previous study showed that transfer efficiency of POC to the deep ocean (the ratio of deep POC flux to satellite-derived POC export flux) is greatest in the subtropical gyres, with lower values at high latitudes (12). This was attributed to organic material exported from low-latitude, carbonate-dominated regions being subject to less remineralization due to ballasting by CaCO₃; to the more refractory nature of the exported material; and to packaging of the material into more hydrodynamic fecal pellets. In contrast, in high-latitude, opal-dominated regions, it was argued that a higher fraction of material was exported, but its more labile nature, combined with less-dense packaging in loose aggregates, was hypothesized to result in the observed lower transfer efficiency to the deep ocean. In another study, also based on deep sediment traps and using thorium-derived export data (28), the greater transfer efficiency and lower *b* values at low latitudes were predominantly attributed to the greater degree of recycling in the upper ocean before export.

We applied the relationship between upper water column temperature and *b* described by this data set (Fig. 2A) to World Ocean Atlas climatology data for the upper 500 m of the water column (29) to give a global distribution of *b* values (Fig. 3, Upper), with the caveat that neither the North Atlantic sites for which we report POC flux nor those sampled during the VERTIGO study were areas characterized by anoxic or suboxic conditions, and so the influence of low oxygen conditions on POC flux attenuation is not represented. Previous studies in such areas (20, 30) suggest that suboxic conditions result in lower *b* values. Assuming that the relationship described here is due to the rate of heterotrophic respiration of sinking POC, in regions of low oxygen concentrations, this effect may therefore act

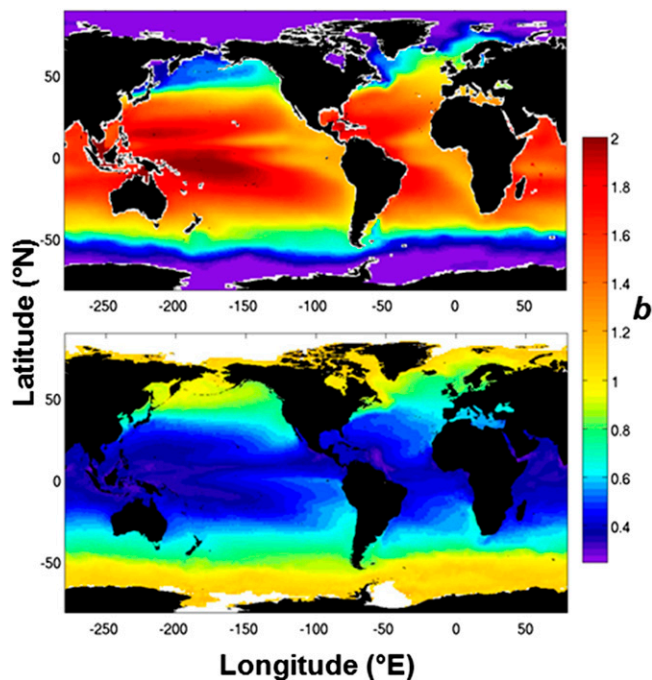


Fig. 3. Global maps of *b* values from (Upper) the relationship between mesopelagic POC flux attenuation and upper water column (500 m) median temperature applied to World Ocean Atlas climatological data (29) and from (Lower) application of algorithms to satellite data, based on studies of thorium-derived POC export and POC flux to deep-sea sediment traps (adapted from ref. 28).

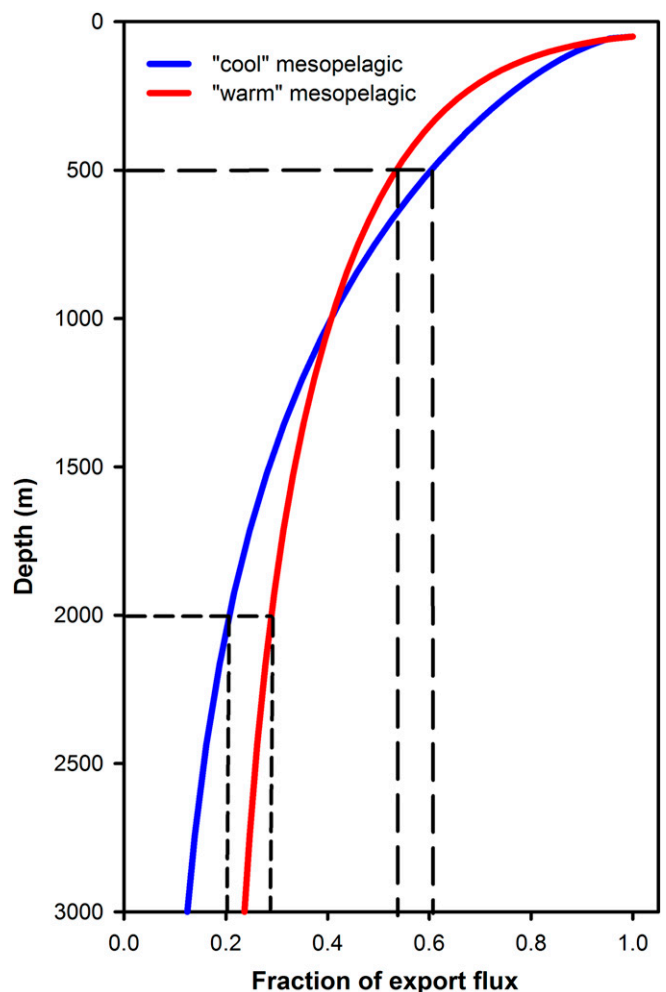


Fig. 4. Conceptual comparison of POC flux profiles in areas with warm (red line) or cool (blue line) mesopelagic waters. In cooler waters, a smaller fraction of exported POC is remineralized in the upper water column (long-dashed lines from 500 m depth), but the nature of the material results in a greater fraction being remineralized before reaching the deep sea (short-dashed lines at 2,000 m), and vice versa in warm waters.

against the attenuation profile predicted by water column temperature. The distribution of *b* values that results from applying the observed relationship to temperature climatology data is strikingly different than the corresponding plot produced using satellite-derived estimates of export and deep-sea POC fluxes (28) (redrawn in Fig. 3, Lower) and highlights the importance of the depth range over which POC flux attenuation is considered. Comparison of the two plots suggests that reliance upon deep-sea trap data will misrepresent POC flux attenuation in the upper few hundred meters of the water column, a depth interval of significant change in vertical flux.

We attempt to reconcile the two approaches conceptually in Fig. 4. The studies based on deep-sea sediment traps each refer to a low export ratio for warm waters, due to efficient recycling of material in the surface mixed layer, but high transfer efficiency of the remaining relatively refractory material (with a high export ratio but lower transfer efficiency at higher latitudes) (12, 28). We suggest rather that in warmer waters, the higher temperatures support higher rates of heterotrophic respiration, which continue to rapidly attenuate POC flux as it sinks through the first few tens to hundreds of meters below the base of the euphotic layer, with little change thereafter. In areas where the

upper water column is relatively cold, remineralization is slower over the upper part of the water column, but the more labile nature of the exported material ultimately results in a greater fraction being remineralized before it reaches abyssal depths. This feature of POC flux depth profiles is missed when considering only export flux and deep-sea sediment trap data.

The contrasting distributions of b in Fig. 3 and the proposed explanation in Fig. 4 suggest that the use of a single mathematical function such as the customary Martin equation may be oversimplified in its description of POC flux attenuation over the whole water column. A more complete description may consider two fractions of POC flux, the relative contributions of which would determine the shape of the flux profile. Such a concept has been suggested in previous studies that have sought to better constrain changes in POC flux over the entire water column (4, 5, 18). Potential mechanisms to partition the POC flux in this way may include consideration of a labile fraction of POC flux and a refractory and/or mineral-ballasted fraction (4). Alternatively, changes in flux through the mesopelagic may largely represent temperature-dependent remineralization of a slow-sinking fraction, while a fast-sinking fraction supplies flux to the deep ocean (31).

Although the data set used in this study is necessarily small, due to the relatively recent availability of NBSTs and the strict stipulation of using only data from studies where POC flux measurements from three or more mesopelagic trap depths are available, the observed relationship between flux attenuation and temperature is supported by laboratory studies that show temperature dependence of carbon-specific respiration rates in plankton communities, diatom aggregates, and bulk POC (25, 27, 32). The fact that a significant relationship with temperature is shown using both the Martin power law and the alternative, less depth-sensitive, exponential function gives confidence that the relationships reported here provide an opportunity to estimate the remineralization depth of sinking organic material based on the relatively straightforward measurement of temperature over the upper water column. This approach would facilitate the estimation of large-scale variability in biological carbon pump efficiency in the mesopelagic ocean—the zone of greatest change in POC flux magnitude. It also offers the potential for b (or z^b) to be included in global biogeochemical models as a more dynamic parameter than it currently is. Furthermore, the relationship supports previous model simulations (2, 19) in suggesting that a warming ocean, resulting from climate change associated with increasing atmospheric CO_2 concentrations, will result in reduced penetration of POC into the water column. This in turn would reduce the capacity of the oceans to store CO_2 , effectively acting as a positive feedback mechanism.

Materials and Methods

Sample Collection. Sampling was carried out during three North Atlantic research cruises (Fig. 1A and *SI Text*), with all sediment traps deployed below the surface mixed layer, as determined from conductivity-temperature-depth (CTD) measurements. At the PAP site (mixed layer depth of 49 m), five PELAGRA traps sampled concurrently at depths between 51 m and 589 m for

48 h, while deployments of three traps each were carried out in the Irminger Basin (20 m mixed layer depth) and Iceland Basin (30 m mixed layer depth), sampling at depths between 80 m and 400 m for periods of 40–50 h in each case. A total of 10 successful trap deployments were carried out over a period of three and a half weeks in the North Atlantic subtropical gyre (mixed layer depth of 45 m), with sampling durations of 72–96 h and at depths between 70 m and 750 m. Full deployment details are given in [Table S1](#).

Sample Processing. Before deployment, sample cups were filled with a brine solution poisoned with chloroform (D341) or formalin (D354, D369). Following trap recovery, sample cups were quickly removed from each trap and processed within 48 h. Initial processing for each trap involved the contents of at least two sample cups being combined and their contents passed through a 350- μm screen to remove zooplankton “swimmers.” The brine/particle mixture was then split into eight subsamples using a custom-built rotary splitter (16). At least one subsample from each trap was dedicated for analyses of each of POC, opal, CaCO_3 , and trace elements, including aluminum (Al). In some cases, as many as three subsamples were designated for one of these components, to make replicate determinations of their totals. Subsamples were filtered while at sea, and the filters were stored frozen (-20°C) until they could be further processed on shore.

Analyses. Samples for POC analysis were treated by established protocols (33) and analyzed using a Thermo Finnigan Flash EA1112 Elemental Analyzer (D341, D354) or a HEKAtech GmbH EURO EA CHNSO Elemental Analyzer (D369). POC mass flux was converted to flux of POM by a multiplicative factor of 2.2 (18). Splits for CaCO_3 were prepared by dissolution with 2% nitric acid, with calcium content measured by inductively coupled plasma optical emission spectrometry (Perkin-Elmer Optima 4300DV ICP-OES) (34) and used to calculate mass of CaCO_3 . Filters for biogenic silica determination were treated with a 0.2-M sodium hydroxide dissolution step, followed by neutralization with hydrochloric acid (35) and subsequent measurement of dissolved silicate by a SEAL Analytical QuAAtro AutoAnalyzer. Results were converted to mass of opal by assuming a water content for opal of 10% (18). Material from trace element splits were subjected to an acetic acid leach followed by digestion with nitric and hydrofluoric acids at 130°C , with residues from each treatment redissolved in 2% nitric acid and analyzed by inductively coupled plasma-mass spectrometry (Thermo Fisher Scientific Element 2 XR HR-ICP-MS). The sum of leach and digest Al fractions were used to calculate a mass of lithogenic material based on an average crustal abundance of 7.96% Al by weight (36).

Temperature Measurements. Median temperatures of the upper 500 m of the water column at each location were calculated using data from CTD deployments carried out near the trap deployments during each research cruise. For VERTIGO stations in the North Pacific, data were accessed from the Ocean Carbon and Biogeochemistry Data Management Office (ocb.whoi.edu/jg/dir/OCB/VERTIGO/).

ACKNOWLEDGMENTS. We are grateful to Sam Ward and Kevin Saw for coordinating PELAGRA deployments and to Peter Statham for his advice and assistance during D341. We gratefully acknowledge the assistance of Mike Zubkov, principal investigator of RRS *Discovery* cruise D369, and the scientists, officers, and crew of all three research cruises, particularly all those who helped as spotters for postdeployment sediment traps. The funding for this work was through Oceans 2025 and Natural Environment Research Council Grant NE/E006833/1 (awarded to E.P.A. and R.J.S.).

- Parekh P, Dutkiewicz S, Follows MJ, Ito T (2006) Atmospheric carbon dioxide in a less dusty world. *Geophys Res Lett* 33(3):L03610.
- Kwon EY, Primeau F, Sarmiento JL (2009) The impact of remineralization depth on the air-sea carbon balance. *Nat Geosci* 2(9):630–635.
- Suess E (1980) Particulate organic carbon flux in the oceans: Surface productivity and oxygen utilization. *Nature* 288(5788):260–263.
- Armstrong RA, Lee C, Hedges JI, Honjo S, Wakeham SG (2002) A new, mechanistic model for organic carbon fluxes in the ocean based on the quantitative association of POC with ballast minerals. *Deep Sea Res Part II* 49(1-3):219–236.
- Lutz M, Dunbar R, Caldeira K (2002) Regional variability in the vertical flux of particulate organic carbon in the ocean interior. *Global Biogeochem Cycles* 16(3):1037.
- Boyd PW, Trull TW (2007) Understanding the export of biogenic particles in oceanic waters: Is there consensus? *Prog Oceanogr* 72(4):276–312.
- Martin JH, Knauer GA, Karl DM, Broenkow WW (1987) VERTEX: Carbon cycling in the northeast Pacific. *Deep Sea Res A* 34(2):267–285.
- Sarmiento JL, Le Quéré C (1996) Oceanic carbon dioxide uptake in a model of century-scale global warming. *Science* 274(5291):1346–1350.
- Lampitt RS, Antia AN (1997) Particle flux in deep seas: Regional characteristics and temporal variability. *Deep Sea Res Part I* 44(8):1377–1403.
- Honjo S, Manganini SJ, Krishfield RA, Francois R (2008) Particulate organic carbon fluxes to the ocean interior and factors controlling the biological pump: A synthesis of global sediment trap programs since 1983. *Prog Oceanogr* 76(3):217–285.
- Berelson WM (2001) The flux of particulate organic carbon into the ocean interior: A comparison of four U.S. JGOFS regional studies. *Oceanography* 14(4):59–67.
- Francois R, Honjo S, Krishfield R, Manganini S (2002) Factors controlling the flux of organic carbon to the bathypelagic zone of the ocean. *Global Biogeochem Cycles* 16(4):1087.
- Buesseler KO, et al. (2007) Revisiting carbon flux through the ocean's twilight zone. *Science* 316(5824):567–570.
- Valdes JR, Price JF (2000) A neutrally buoyant, upper ocean sediment trap. *J Atmos Ocean Technol* 17(1):62–68.
- Buesseler KO, et al. (2008) VERTIGO (VERTical Transport In the Global Ocean): A study of particle sources and flux attenuation in the North Pacific. *Deep Sea Res Part II* 55(14-15):1522–1539.

16. Lamborg CH, et al. (2008) The flux of bio- and lithogenic material associated with sinking particles in the mesopelagic "twilight zone" of the northwest and North Central Pacific Ocean. *Deep Sea Res Part II* 55(14-15):1540–1563.
17. Boyd PW, Newton PP (1999) Does planktonic community structure determine downward particulate organic carbon flux in different oceanic provinces? *Deep Sea Res Part I* 46(1):63–91.
18. Klaas C, Archer DE (2002) Association of sinking organic matter with various types of mineral ballast in the deep sea: implications for the rain ratio. *Global Biogeochem Cycles* 16(4):1116.
19. Matsumoto K (2007) Biology-mediated temperature control on atmospheric pCO_2 and ocean biogeochemistry. *Geophys Res Lett* 34(20):L20605.
20. Devol AH, Hartnett HE (2001) Role of the oxygen-deficient zone in transfer of organic carbon to the deep ocean. *Limnol Oceanogr* 46(7):1684–1690.
21. Buesseler KO, Boyd PW (2009) Shedding light on processes that control particle export and flux attenuation in the twilight zone of the open ocean. *Limnol Oceanogr* 54(4):1210–1232.
22. Lampitt RS, et al. (2008) Particle export from the euphotic zone: Estimates using a novel drifting sediment trap, ^{234}Th and new production. *Deep Sea Res Part I* 55(11):1484–1502.
23. Alonso-González IJ, et al. (2010) Role of slowly settling particles in the ocean carbon cycle. *Geophys Res Lett* 37(13):L13608.
24. Trull TW, et al. (2008) *In situ* measurement of mesopelagic particle sinking rates and the control of carbon transfer to the ocean interior during the Vertical Flux in the Global Ocean (VERTIGO) voyages in the North Pacific. *Deep Sea Res Part II* 55(14-15):1684–1695.
25. Iversen MH, Ploug H (2013) Temperature effects on carbon-specific respiration rate and sinking velocity of diatom aggregates – potential implications for deep ocean export processes. *Biogeosciences* 10(6):4073–4085.
26. Rivkin RB, Legendre L (2001) Biogenic carbon cycling in the upper ocean: Effects of microbial respiration. *Science* 291(5512):2398–2400.
27. Wohlers J, et al. (2009) Changes in biogenic carbon flow in response to sea surface warming. *Proc Natl Acad Sci USA* 106(17):7067–7072.
28. Henson SA, Sanders R, Madsen E (2012) Global patterns in efficiency of particulate organic carbon export and transfer to the deep ocean. *Global Biogeochem Cycles* 26(1):GB1028.
29. Locarnini RA, et al. (2010) *Temperature*, World Ocean Atlas 2009 (U.S. Gov Printing Off, Washington, DC), Vol 1.
30. Van Mooy BAS, Keil RG, Devol AH (2002) Impact of suboxia on sinking particulate organic carbon: Enhanced carbon flux and preferential degradation of amino acids via denitrification. *Geochim Cosmochim Acta* 66(3):457–465.
31. Riley JS, et al. (2012) The relative contribution of fast and slow sinking particles to ocean carbon export. *Global Biogeochem Cycles* 26(1):GB1026.
32. Bendtsen J, Hilligsøe KM, Hansen JLS, Richardson K (2015) Analysis of remineralisation, lability, temperature sensitivity and structural composition of organic matter from the upper ocean. *Prog Oceanogr* 130:125–145.
33. Salter I, et al. (2007) Estimating carbon, silica and diatom export from a naturally fertilised phytoplankton bloom in the Southern Ocean using PELAGRA: A novel drifting sediment trap. *Deep Sea Res Part II* 54(18-20):2233–2259.
34. Green DRH, Cooper MJ, German CR, Wilson PA (2003) Optimization of an inductively coupled plasma-optical emission spectrometry method for the rapid determination of high-precision Mg/Ca and Sr/Ca in foraminiferal calcite. *Geochem Geophys Geosyst* 4(6):8404.
35. Brown L, Sanders R, Savidge G, Lucas CH (2003) The uptake of silica during the spring bloom in the Northeast Atlantic Ocean. *Limnol Oceanogr* 48(5):1831–1845.
36. Wedepohl KH (1995) The composition of the continental crust. *Geochim Cosmochim Acta* 59(7):1217–1232.